

2

REPORT DOCUMENTATION PAGE

Form Approved
OMB No. 0704-0188

Public reporting burden for this collection of information is estimated to average 1 hour per response, including the time for reviewing instructions, searching existing data sources, gathering and maintaining the data needed, and completing and reviewing the collection of information. Send comments regarding this burden estimate or any other aspect of this collection of information, including suggestions for reducing this burden, to Washington Headquarters Services, Directorate for Information Operations and Reports, 1215 Jefferson Davis Highway, Suite 1204, Arlington, VA 22202-4302, and to the Office of Management and Budget, Paperwork Reduction Project (0704-0188), Washington, DC 20503.

1. AGENCY USE ONLY (Leave blank)

2. REPORT DATE

July 25, 1995

3. REPORT TYPE AND DATES COVERED

Technical Report 06/01/94 - 05/31/95

4. TITLE AND SUBTITLE

Thermoconvection-enhanced deposition of copper.

5. FUNDING NUMBERS

Grant: N00014-93-1-0375-1

R&T Code: 3133043

Dr. Robert J. Nowak

6. AUTHOR(S)

Nick Isaev and Janet G. Osteryoung

7. PERFORMING ORGANIZATION NAME(S) AND ADDRESS(ES)

North Carolina State University
Office of Sponsored Programs
Box 7514
Raleigh, NC 27695-7514

8. PERFORMING ORGANIZATION
REPORT NUMBER

Technical Report No.2

9. SPONSORING / MONITORING AGENCY NAME(S) AND ADDRESS(ES)

Office of Naval Research
Chemistry Division
800 North Quincy Street
Arlington, VA 22217-5660

10. SPONSORING / MONITORING
AGENCY REPORT NUMBER

11. SUPPLEMENTARY NOTES

For publication in The Journal of The Electrochemical Society.

12a. DISTRIBUTION / AVAILABILITY STATEMENT

Reproduction in whole, or in part, is permitted for any purpose of the United States Government. This document has been approved for public release and sale; its distribution is unlimited.

12b. DISTRIBUTION CODE

13. ABSTRACT (Maximum 200 words)

Thermal gradients and thermoconvective flow in the vicinity of the electrode are shown to enhance mass-transport of the electroactive species during reduction of copper. The transport-limited current of the copper reduction reaction is more than doubled under conditions of positive and negative thermal gradient in comparison with isothermal conditions. Furthermore, thermal gradients affect strongly the potential dependence of the current.

Kinetic and thermodynamic parameters for electrodeposition of copper were determined from polarization curves analyzed with Butler-Volmer, Tafel, and Levich expressions. Under isothermal conditions the exchange current density for the copper reduction reaction was found to be given by $\log i_0 = 7.95 - 2690T^{-1}$ (i_0 in mA cm⁻² and T in K) under conditions of 10 mM CuSO₄ in 2 M H₂SO₄ ($10 \leq T/^\circ\text{C} \leq 80$). The diffusion coefficient of Cu(II) at 298 K under the same conditions was found to be $5.36 \cdot 10^{-6}$ cm² s⁻¹.

Decrease of the effective thickness of the diffusion layer due to thermoconvection in the vicinity of the cathode is responsible for the effect of the gradient on transport-limited current.

14. SUBJECT TERMS

Convection, thermal gradient, copper, electrodeposition, corrosion

15. NUMBER OF PAGES

28

16. PRICE CODE

17. SECURITY CLASSIFICATION
OF REPORT

Unclassified

18. SECURITY CLASSIFICATION
OF THIS PAGE

Unclassified

19. SECURITY CLASSIFICATION
OF ABSTRACT

Unclassified

20. LIMITATION OF ABSTRACT

NSN 7540-01-280-5500

Standard Form 298 (Rev 2-89)
Prescribed by ANSI Std Z39-18
298-112

19950814 006

JGK

OFFICE OF NAVAL RESEARCH

GRANT: N00014-93-1-0375-1

R&T Code 3133043

Technical Report No. 2

Thermoconvection-Enhanced Deposition of Copper

by

Nick Isaev and Janet G. Osteryoung

Prepared for Publication

in the

Journal of The Electrochemical Society

North Carolina State University
Department of Chemistry
Raleigh, NC 27695-8204

July 25, 1995

Reproduction in whole or in part is permitted for any purpose of the United States
Government.

This document has been approved for public release and sale; its distribution is unlimited.

Thermoconvection-enhanced deposition of copper

Nick Isaev and Janet G. Osteryoung

Department of Chemistry

North Carolina State University

Raleigh, North Carolina, 27695-8204

Accession For	
NTIS GRA&I	<input checked="checked" type="checkbox"/>
DTIC TAB	<input type="checkbox"/>
Unannounced	<input type="checkbox"/>
Justification	
By	
Distribution/Avail	
Availability Codes	
Avail and/or	Special
None	
A-1	

Abstract

Thermal gradients and thermoconvective flow in the vicinity of the electrode are shown to enhance mass-transport of the electroactive species during reduction of copper. The transport-limited current of the copper reduction reaction is more than doubled under conditions of positive and negative thermal gradient in comparison with isothermal conditions. Furthermore, thermal gradients affect strongly the potential dependence of the current.

Kinetic and thermodynamic parameters for electrodeposition of copper were determined from polarization curves analyzed with Butler-Volmer, Tafel, and Levich expressions. Under isothermal conditions the exchange current density for the copper reduction reaction was found to be given by $\log i_0 = 7.95 - 2690T^{-1}$ (i_0 in mA cm^{-2} and T in K) under conditions of 10 mM CuSO_4 in 2 M H_2SO_4 ($10 \leq T/^{\circ}\text{C} \leq 80$). The diffusion coefficient of Cu(II) at 298 K under the same conditions was found to be $5.36 \cdot 10^{-6} \text{ cm}^2 \text{ s}^{-1}$.

Decrease of the effective thickness of the diffusion layer due to thermoconvection in the vicinity of the cathode is responsible for the effect of the gradient on transport-limited current.

Introduction

Microfabrication of electronic systems often requires the deposition and electrochemical etching of a metal film that is covered by a photoresist mask. In such a case, the electrode layout is determined photolithographically so that deposited features are within the size domain of the microprofile. These processes are mass-transport limited by diffusion of the active components to the electrode surface or away from the reactive zone. A key feature in these technologies is a close relationship between the hydrodynamic conditions in the immediate vicinity of the electrode and the mass-transport rate. Physicochemical hydrodynamics [1] or free convection [2], which is due to variations of the concentration of reactant species during the electrochemical reaction, has been studied by many investigators [2-6].

The specific focus of this work was prompted by reports of local increase of current density during laser-enhanced plating [7-11]. A model for this process has been proposed [7]. The increased reaction rate in the presence of laser light is ascribed to an increase of temperature at the metal-solution interface, which has three separate effects. First, there is strong microstirring of the solution due to thermal gradients, with additional stirring at high laser power densities due to local boiling of the solution. Second, there is an increase in the charge transfer rate with increase in temperature. Third, the standard potential for the process depends on the temperature. The factors which influence laser-enhanced copper plating and the mechanism of this enhancement have been studied [8,11], as has the effect of local boiling [9,10]. Other works on this subject have been dedicated

to the calculation of heat and mass-transport parameters during the electrodeposition process under conditions of laser illumination [9,12].

Our specific objective was to investigate the effect of an imposed thermal gradient in the vicinity of the electrode on the electrochemical deposition reactions of copper. Our focus is on conditions appropriate to the problem of electrodeposition. It should be noted, however, that other important practical systems are strongly affected by thermal gradients. For example, wet corrosion of copper is subject to this phenomenon, which may affect the corrosion process through change in kinetic and thermodynamic properties, including product distribution, and in mass-transport [13]. This work is most clearly related to the behavior of copper heating or cooling coils.

The problem

Figure 1 presents a simple scheme of the electrode-solution interface during the electrodeposition process. The concentration of the reacting species changes from the bulk concentration (C_b) to zero within the diffusion layer (δ_c) (curve 1, fig. 1). It is reasonable to hypothesize that a thermal layer (δ_T) also exists near the electrode when the solution and electrode have different temperature. By convention, when the temperature of the electrode (T_E) is greater than the temperature of the solution (T_S), there is a positive thermal gradient (curve 2, fig. 1). A negative thermal gradient exists when T_S is higher than T_E (curve 3, fig. 1).

The electrochemical reactions of metal deposition usually include as parts of the process transport of reactants to the cathode by diffusion and convection, the charge transfer process, and an electrocrystallization step. (We consider the case of a simple reduction reaction in a supporting electrolyte without any chemical reaction in solution and no adsorption effects on the surface of the electrode.) Temperature variations play an important role in each part of the overall process. They change mass-transport conditions, because diffusion coefficients of species and the viscosity and density of the electrolyte depend on the temperature. They influence the thermodynamic and kinetic parameters of the electrochemical reaction, since the standard potential, rate constant, overvoltage and probably transfer coefficient also depend on the temperature. They change the parameters of the electrocrystallization step, since the size and number of nuclei depend on the overvoltage and the latter, in turn, depends on the temperature.

The main goal of this work was the experimental investigation of the copper reduction reaction under conditions of a temperature gradient across the electrode-solution interface. We employed an electrode with the temperature controlled independently from the temperature of the solution. The thermal gradient in the vicinity of the electrode generates a strong laminar or even turbulent flow, which is due to fluctuations of the viscosity and density of the electrolyte. It is very difficult to define potential, concentration and thermal profiles in the region near the electrode, where diffusion and convective transport contribute roughly equally to the mass-transport rate. Systems of such complexity reveal the arbitrary nature of the customary division of transport processes into diffusion and convection.

Experimental details

Instrumentation. Electrochemical measurements were performed with a Model 273 potentiostat (EG&G PARC). For controlling the cell and electrode temperature in the range of 10 - 80 °C, two circulating systems (HAAKE FE2 and GCA Precision Scientific Company) and a portable cooler (Precision Scientific Company) were used. The Ring-Disk Electrode System (EG&G PARC) Model 636 was used for all rotating disk experiments.

Materials. Reagents were reagent grade. The stock solution of Cu(II) was prepared by the dissolution of anhydrous CuSO₄ in water, the addition of an equimolar amount of H₂SO₄ (to make a 2 M solution) and diluting to volume with water. Water from the house ion exchange supply was passed through a four-cartridge Millipore Milli-Q purification system. Solutions were deaerated by purified argon for 1 h before use.

Electrodes and cell. The Pt stationary electrode was machined so that a microcooler could be embedded in the electrode from the back as shown in Figure 2. This construction makes it possible to control the temperature of the working electrode. Area of this electrode was 0.164 cm².

The reference electrode was a copper wire immersed in the solution of the working electrolyte. The potentials were measured with respect to the Cu(II)/Cu⁰ redox couple in the same electrolyte. The temperature of the reference electrode conformed to the solution temperature. The electrode for the rotating disk experiment was a Pine AFMR28PTPT RDE (disk area is 0.164 cm²). The counter electrode was a Pt wire of large surface area.

All measurements were performed in a standard electrochemical cell which was made of glass and had three compartments, one for the reference electrode and the other two for the working and the counter electrodes.

Procedures. Three different types of temperature regimes were employed: (1) isothermal conditions, where temperatures of the solution and electrode were the same and were varied from 20 to 80 °C; (2) conditions of negative thermal gradient, when the solution temperature was varied from 30 to 60 °C and the temperature of the electrode was 20 - 50 °C lower than the temperature of the solution; (3) conditions of positive thermal gradient, when the temperature of the solution was constant (10 °C) and the electrode temperature was 20 - 60 °C higher than the temperature of the solution.

Platinum stationary and rotating disk electrodes were polished before each series of experiments using microcloth polishing cloths and suspensions of alumina powder down to 0.05 μm .

Copper was deposited on the Pt electrode for 5 min before obtaining each polarization curve. The deposition potential was -0.3 V vs. the copper reference electrode. After deposition, the electrodes were polarized at +0.04 V for 30 s, and then quasi-steady-state polarization curves were obtained by scanning the potential at the rate of 1 mV s⁻¹. These experiments were done under conditions of thermal gradients using the apparatus of Figure 2.

Kinetic and diffusional parameters were obtained under isothermal conditions using the rotating disk electrode in the usual fashion. Plots of transport-limited current

against square-root of rotation rate were used to obtain the diffusion coefficient of Cu(II), and inverse plots were used to obtain potential-dependent currents, corrected for transport, which then were used to calculate exchange current density. The range of rotation rate employed was 500 - 2500 rpm.

Results and discussion

Current-voltage curves for the deposition and dissolution of copper obtained under isothermal conditions and under conditions of positive and negative thermal gradients as described above are shown in Figure 3. At sufficiently negative potentials the cathodic current is transport-limited. Current-potential dependencies and values of transport-limited currents reflect changes in kinetic and mass-transport parameters of the copper reduction-oxidation reaction with change in temperature and temperature-gradient. An increase of temperature from 20 to 70 °C under isothermal conditions (Figure 3, curves 3 and 4) increases the reaction rate by a factor of 4.8 in the potential-independent region. In the case of a positive thermal gradient (Figure 1, curve 2), the transport-limited current increases more than 8.5 times when the temperature of the electrode increases from 30 to 70 °C. A completely different response is observed under a negative thermal gradient (Figure 3, curve 1). In this case, over the same range of potentials, the cathodic reaction appears kinetically controlled and the transport-limited current is close to potentials of hydrogen evolution. Recall that the reference electrode is at the temperature of the solution, so curves 1 and 3 have the same reference potential, whereas the reference

potential for curves 2 and 4 is shifted according to the temperature dependence of the standard potential for the Cu(II)/Cu(0) couple.

The increase in transport-limited current when there is a temperature differential in the system can result from changing diffusion conditions and by microstirring due to thermal gradients near the electrode-solution interface. Variation of temperature leads to changes in the diffusion layer thickness, because the diffusion coefficient of Cu(II) changes according to Arrhenius' law and the kinematic viscosity of the electrolyte also varies. On the other hand, the fluctuation in density of the solution due to thermal gradients leads to microstirring near the cathode, which decreases the thickness of the diffusion layer.

The total flux density for the reacting species (N) may be expressed as the sum of three main components:

$$N = N_D + N_C + N_T \quad (1)$$

where N_D is the diffusion flux, N_C is the convective flux, and N_T is the thermodiffusion flux. Thermodiffusion can be characterized by the Soret coefficient (σ), which describes the movement of solvent or electrolyte to areas with higher temperature. The Soret coefficient is defined as $(1/C) \partial C / \partial T$ [14]. In the case at hand, the major effect of thermodiffusion is the dilution of Cu(II) by thermodiffusion of sulfuric acid to the hotter zone. Thus the measured current is smaller than the current corrected for thermodiffusion when the temperature gradient is positive. The thermodiffusion current, i_T , was calculated according to

$$i_T = i_L(T_C) \sigma (T_E - T_S) \quad (2)$$

where i_L is the isothermal transport-limited current at the effective temperature, T_C , discussed below. The value of the Soret coefficient for sulfuric acid under these conditions is -0.0049 K^{-1} [15]. It should be stressed that this treatment is not exact. The magnitude of the correction is large enough (ca. 10%) that it should not be ignored. Inadequate data for Soret coefficients discourages a more elaborate treatment. Calculated values of the thermodiffusion contribution were used to correct transport-limited current for the copper reduction reaction. The corrected total flux density, N' , then includes only two main components:

$$N' = N_D + N_C \quad (3)$$

As shown in Figure 4 the corrected transport-limited current for the copper reduction reaction increases with increasing thermal gradient for both positive (curve 1) and negative (curve 2) gradient. The transport-limited current is linear in the temperature difference in both cases and the slopes are ca $0.015 \text{ mA cm}^{-2} \text{ deg}^{-1}$ for the positive thermal gradient and $0.008 \text{ mA cm}^{-2} \text{ deg}^{-1}$ for the negative thermal gradient

The experimental arrangement fixes reliably the temperature of the electrode and of the solution away from the electrode, whereas the values of parameters that characterize the kinetic and mass-transport properties depend on the temperature in the region where the reaction takes place (Figure 1). In order to estimate that temperature we adopted the following approach. The exchange current density was determined over the temperature range of interest under isothermal conditions, and then it was determined under conditions of thermal gradient. The temperature in the reaction zone was then calculated as the temperature required under isothermal conditions to yield the measured

current density. As the potential and temperature are independently variable, this should yield a reasonable value for the effective temperature under conditions of thermal gradient.

For the conditions of thermal gradient, we employed polarization curves as described in Figure 3. Mass-transfer-corrected Tafel plots were constructed for all polarization curves by using the Butler-Volmer equation for large negative overvoltages, for which the second exponential term becomes negligible:

$$i_c = i_o (1 - i_c / i_L) \exp(-\alpha_c z F \eta / RT) \quad (4)$$

where i_c is the cathodic current density, i_o is the exchange current density, i_L is the transport-limited current density in the cathodic process, α_c is the transfer coefficient for the cathodic process, z is number of electrons, and η is the overvoltage. In this case the cathodic branch of the mass-transfer corrected Tafel plot is described as:

$$\eta = (RT / \alpha_c z F) \{ \ln i_o - \ln [i_c i_L / (i_c - i_L)] \} \quad (5)$$

and the anodic branch is described by:

$$\eta = (RT / \alpha_A z F) \{ \ln i_o - \ln i_A \} \quad (6)$$

where i_A is the anodic current density, and α_A is the transfer coefficient for the anodic process. Exchange current densities were determined from the intersection of cathodic and anodic branches of Tafel plots for each temperature.

Physical and kinetic characteristics of the acid copper sulfate solution were obtained from RDE experiments under isothermal conditions for 298 K. Values of the diffusion coefficient and exchange current density agree with previously measured values, as shown in Table 1. The logarithm of diffusion coefficient depends linearly on reciprocal temperature as expected and shown in Figure 5. The slope, $\partial D / \partial T$, has the value

$(0.16 \pm 0.02) 10^{-10} \text{ m}^2 \text{ s}^{-1} \text{ K}^{-1}$, which agrees well with the value of $0.14 10^{-10} \text{ m}^2 \text{ s}^{-1} \text{ K}^{-1}$, determined by Arvia et al. [20].

The thermal dependence of the exchange current density for the Cu(II)/Cu(0) redox couple was obtained by using data from the RDE experiments analyzed in the usual way. Results are shown in Figure 6. The equation which describes this dependence is

$$\log i_0 (T_i) = 7.95 - 2690 / T \quad (7)$$

Equation 7 is correct for isothermal conditions. Equation 7 was rewritten for the conditions when working and reference electrodes have different temperature:

$$\log i_0 (T_i) = \log i_0 (T_s) + 2690(T_s - T_c) / T_s^2 \quad (8)$$

where T_c is effective temperature in the reactive zone. Equation 8 was inverted and used to calculate, from the exchange currents determined from polarization curves under conditions of thermal gradient, the effective temperature, T_c , in the reaction zone:

$$T_c = T_s + \{ T_s^2 [\log i_0 (T_s) - \log i_0 (T_i)] \} / 2690 \quad (9)$$

The calculated effective temperatures are presented in Table 2. According to this estimate, the temperature is near that of the higher temperature regardless of the sign of the gradient and adopts a more intermediate value when the magnitude of the gradient is larger.

Figure 7 displays the effect of temperature on transport-limited current for the isothermal case (curve 2) and for the case of thermal gradient (curve 1), using the effective temperatures of Table 2 for the latter. Clearly the thermal gradient more than doubles the transport-limited rate, regardless of the direction of the gradient. Furthermore, the effect of the gradient on transport properties is about the same for positive and negative

gradients. That is, the effect on transport of the direction of the gradient is contained mainly in the thermodiffusion, which has been subtracted out.

The temperature dependence of the transport-limited current (Figure 7, curve 1) and the temperature dependence of the diffusion coefficient (Figure 5) make it possible to calculate the effective diffusion layer thickness according to

$$\delta = (zFDC) / i_L \quad (10)$$

by using values of diffusion coefficients and transport-limited currents for the particular temperature in the reaction zone. The results are shown in Figure 8. The thickness of the diffusion layer is decreased by the thermal gradient in comparison with isothermal conditions, and it decreases with increasing of the thermal gradients, either positive or negative, across the electrode-solution interface. This is due to the increase of the convective contribution to the mass-transport rate.

Conclusions

In this work we have shown that positive or negative thermal gradients in the vicinity of the electrode affect both mass-transport and kinetic parameters of the reaction. With respect to mass-transport, the effect of temperature gradient, positive or negative, is to increase the mass-transport-limited current. This increase is due to in part to increase in diffusion coefficient with temperature, and in part to a striking decrease in diffusion layer thickness resulting from the temperature gradient.

The effect on diffusion layer thickness is independent of the direction of the temperature gradient and depends, over the range studied, only slightly on the magnitude of the gradient.

A key feature of this work is the use of the temperature dependence of the reaction rate to estimate temperature. Because the rate is an exponential function of inverse temperature, this is a sensitive way to estimate temperature. Although we do not have an independent assessment of accuracy, the plausibility of the results suggests that this approach is reasonable.

Acknowledgment

This work was supported in part by the Office of Naval Research.

References

1. R. Probstein, in: *Physical Hydrodynamics. An Introduction*, p.1, Butterworth, Boston (1989).
2. J. Selman, J. Newman, *This Journal*, **118**, 1070 (1971).
3. V. Anatharaman, P. Pintauro, L. Nanis, *ibid.*, **136**, 1727 (1989).
4. S. Roy, P. Pintauro, *ibid.*, **140**, 3167 (1993).
5. F. Alavyoon, *Electrochim. Acta*, **37**, 333 (1992).
6. J. Krysa, *J. Appl. Electrochem.*, **22**, 429 (1992).
7. J. Puipe, R. Acosta, R. von Gutfeld, *This Journal*, **128**, 2539 (1981).
8. P. Bindra, G. Abrach, U. Stimming, *ibid.*, **134**, 2893 (1987).
9. H. Kuiken, F. Mikkers, P. Wierenga, *ibid.*, **130**, 554 (1983).
10. J. Jacobs, J. Rikken, *ibid.*, **134**, 2690 (1987).
11. M. Hsiao, C. Wan, *ibid.*, **140**, 1334 (1993).
12. M. Hsiao, C. Wan, *ibid.*, **138**, 2273 (1991).
13. H. Uhlig, R. Revie, *Corrosion and Corrosion Control*, pp. 90-96, John Wiley & Sons, New York (1985).
14. H. Tyrrell, in: *Electrochemical constants*, pp. 119 - 129, Nat. Bur. Std. (U.S.) (1953).
15. C. Tanner, *Trans. Faraday Soc.*, **23**, 75 (1927).
16. C. Milora, J. Henrikson, W. Hahn, *This Journal*, **120**, 488 (1973).
17. I. Burrows, J. Harrison, J. Thompson, *J. Electroanal. Chem.*, **11**, 241 (1975).
18. T. Quickenden, X. Jiang, *Electrochim. Acta*, **29**, 693 (1984).

19. H. Albaya, W. Lorenz.. *Z. Phys. Chem.*, **81**, 294 (1972).
20. A. Arvia, J. Bazan, J. Carrozza, *Electrochim. Acta.*, **11**, 881 (1966).

Table 1.

Physical and electrode kinetic properties of the acid copper sulfate solution ^a

H ₂ SO ₄ / M	10 ⁶ D / cm ² s ⁻¹	i ₀ / mA cm ⁻²	References
1.0	5.23		[16]
1.0	3.95		[17]
2.0	5.36		This work
0.1		0.650	[18]
0.1		0.110	[19]
2.0		0.343	This work

^a 10 mM CuSO₄, 298 K

Table 2 Temperature in the reactive zone ^a.

$T_E / ^\circ\text{C}$	$T_s / ^\circ\text{C}$	$\log i_o(T_i)$ (mA cm ⁻²)	$\log i_o(T_s)$ (mA cm ⁻²)	$T_C / ^\circ\text{C}$
10	30	-0.93	-0.96	28.9
10	40	-0.64	-0.88	31.4
10	50	-0.38	-0.73	36.4
10	60	-0.13	-0.61	40.1
30	10	-1.56	-0.90	29.5
40	10	-1.56	-0.71	35.2
50	10	-1.56	-0.47	42.3
60	10	-1.56	-0.27	48.3
70	10	-1.56	0	56.3

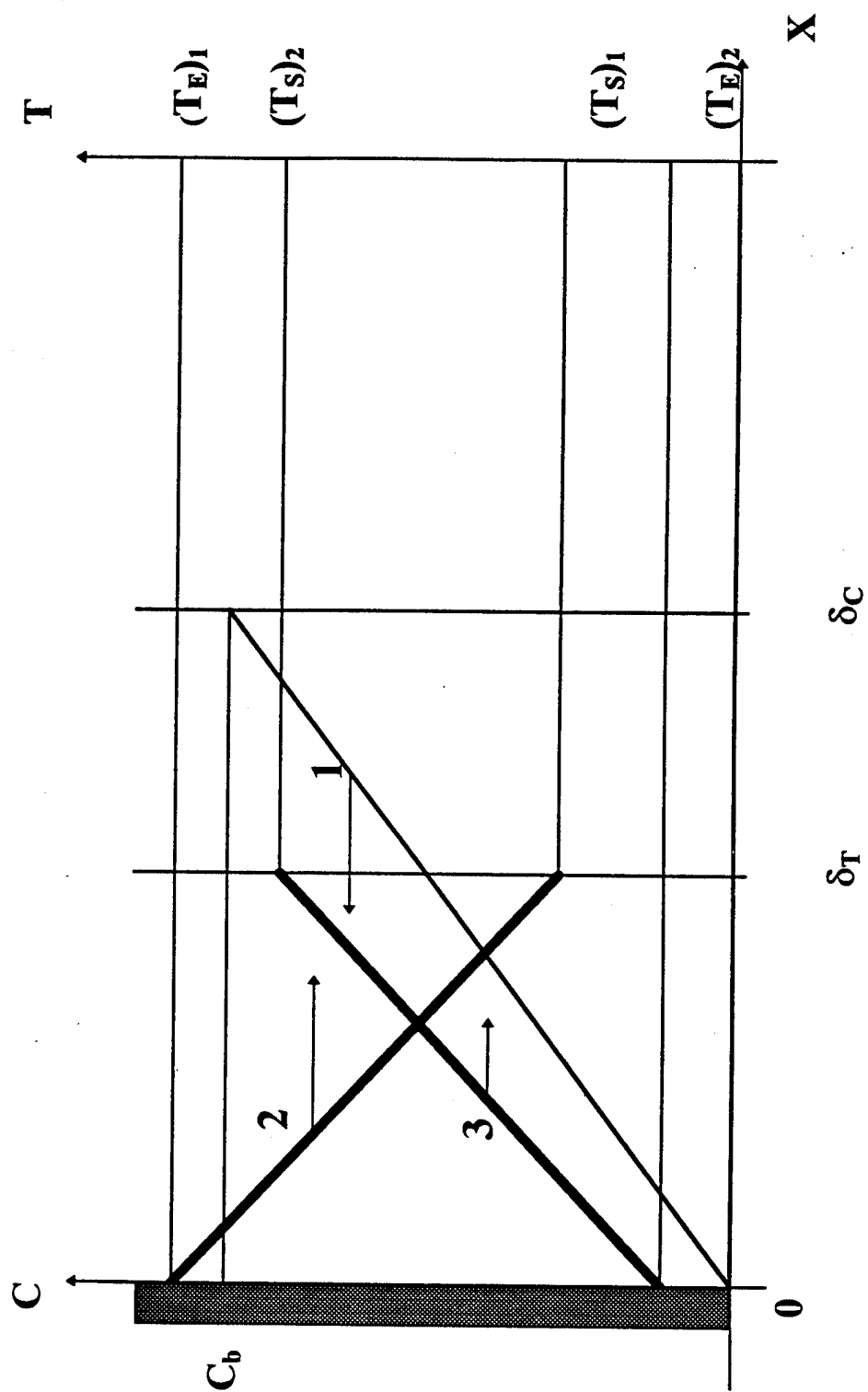
^a calculated from eqn 8

Figure captions

1. The scheme of the electrode-solution interface (reduction reaction). Curve 1 illustrate the concentration gradient and the related diffusion layer thickness, δ_c , and curve 2 and 3 illustrate positive (2) and negative (3) thermal gradients and the related thermal layer thickness, δ_T .
2. The principal scheme of the working electrode.
3. Polarization curves of the copper reduction-oxidation. Solution: CuSO_4 - 5 mM, H_2SO_4 - 2 M. Temperature (°C): 1 (\diamond) - $T_E = 20$, $T_s = 70$ (negative thermal gradient); 2 (x) - $T_E = 70$, $T_s = 20$ (positive thermal gradient); 3 (O) - $T_E = T_s = 70$ (isothermal conditions); 4 (Δ) - $T_E = T_s = 20$ (isothermal conditions). Linear potential scan at 1 mV s^{-1} .
4. Transport-limited current (1, 2), and transport-limited current corrected for thermodiffusion (1', 2'), as a function of thermal gradient. 1 (+), 1' (\diamond) - positive thermal gradient; 2 (x), 2' (O) - negative thermal gradient. Solution as in Figure 3.
5. Thermal dependence of the diffusion coefficient from rotating disk voltammograms. Solution as in Figure 3.
6. Thermal dependence of the exchange current density from rotating disk voltammograms. Solution as in Figure 3.
7. Transport-limited current, corrected for thermodiffusion, as a function of temperature. 1 - measured under conditions of thermal gradient (\diamond - positive, O - negative), transport-limited current as a function of calculated temperature, data of Figure 4 and Table 2; 2 (+) - isothermal conditions, data of Figure 5. Solution as in Figure 3.

8. Calculated diffusion layer thickness as a function of values of thermal gradients from data of Figures 5 and 7. (\diamond) - positive thermal gradient, \circ - negative thermal gradient, (+) - isothermal conditions.

Fig. 1



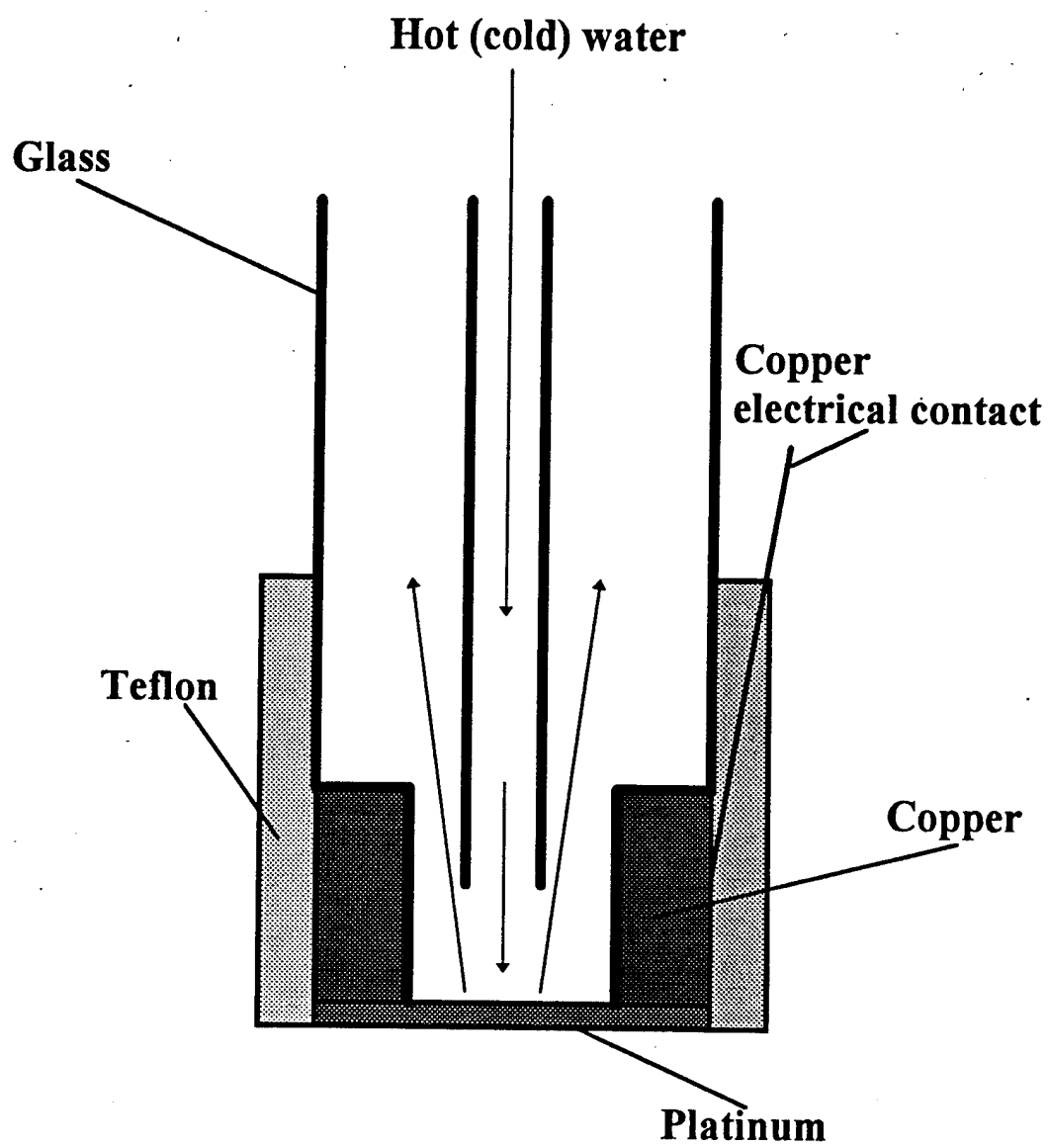


Fig. 3

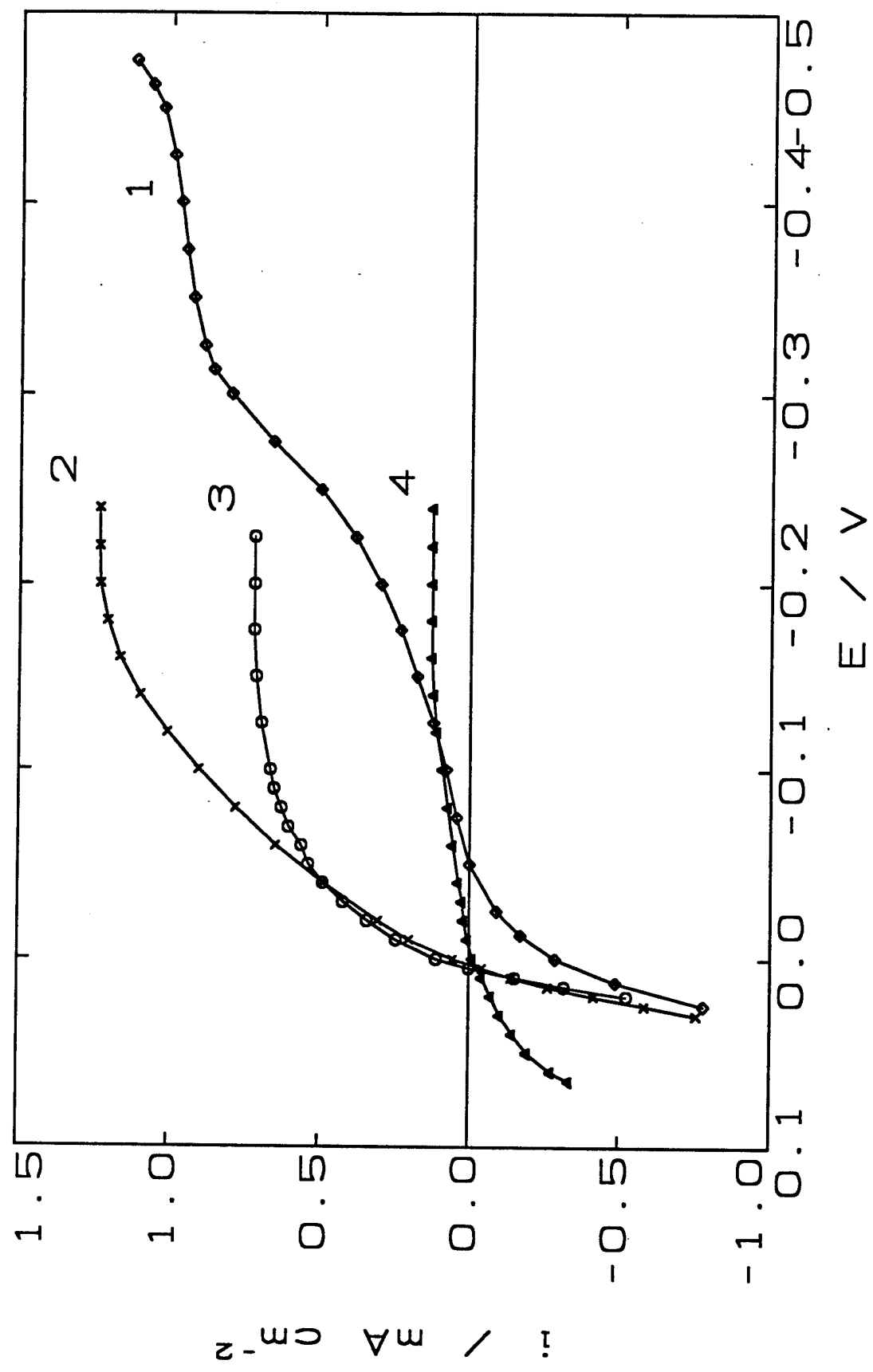


Fig. 4

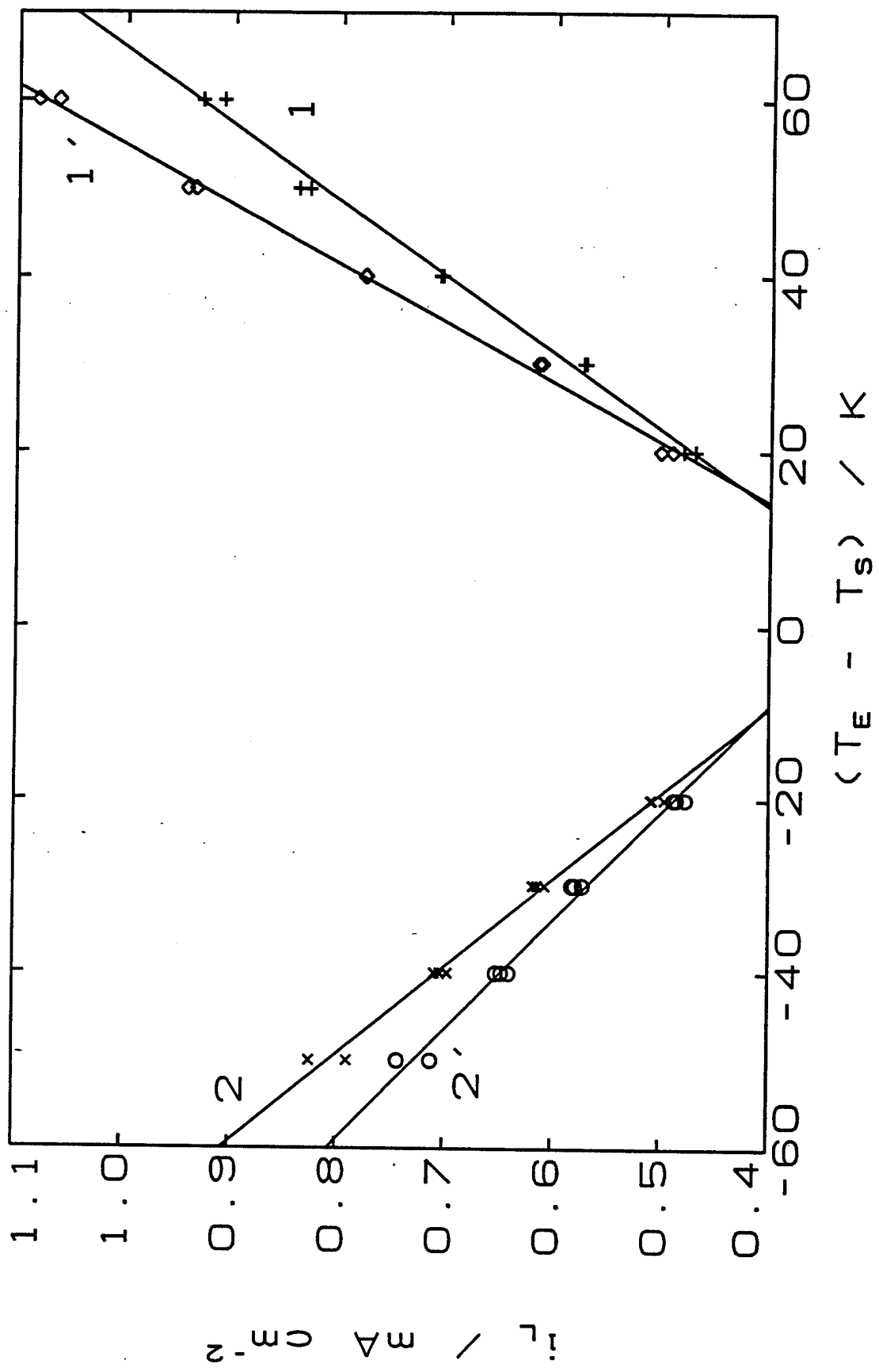


Fig. 5

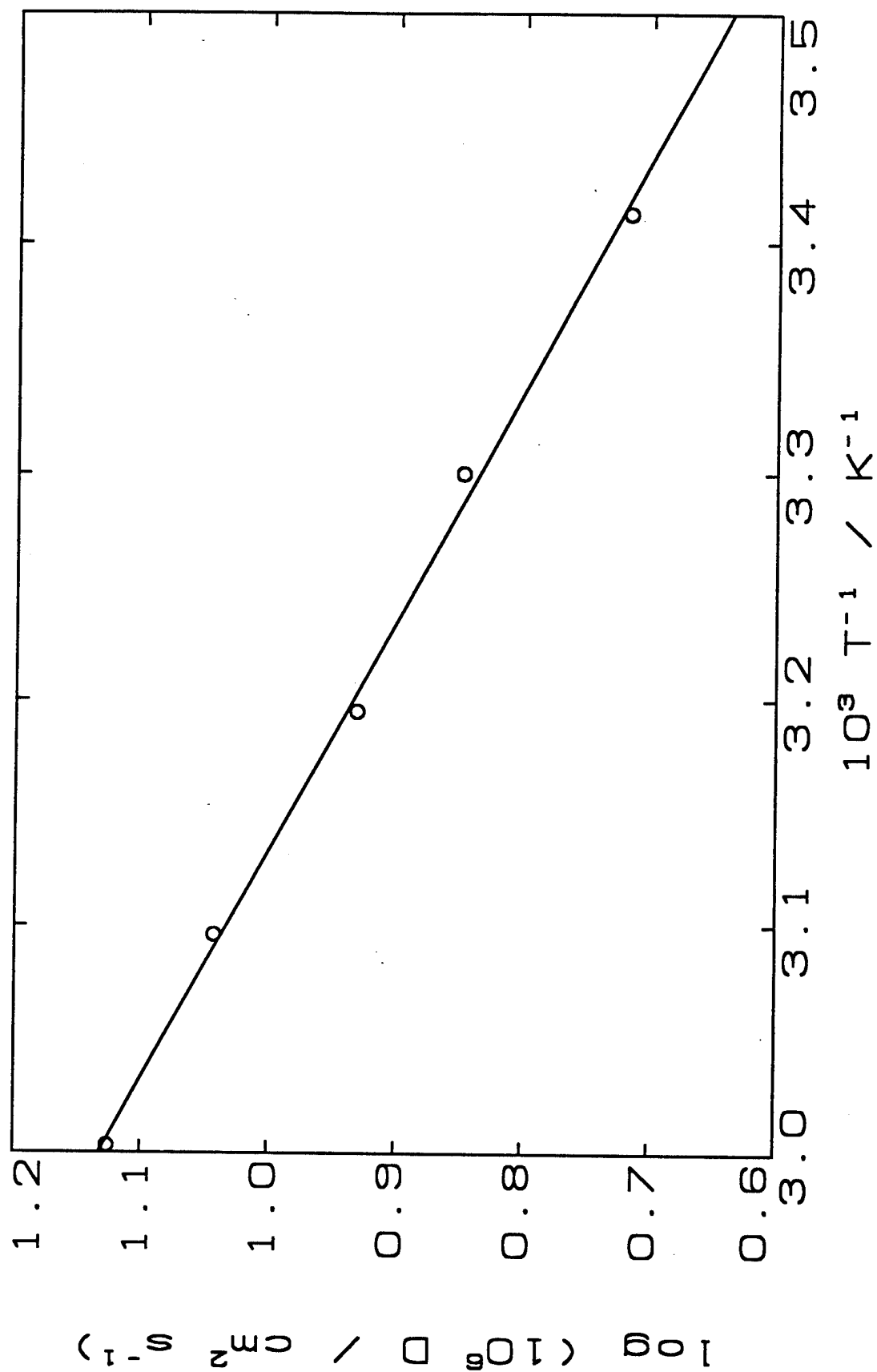
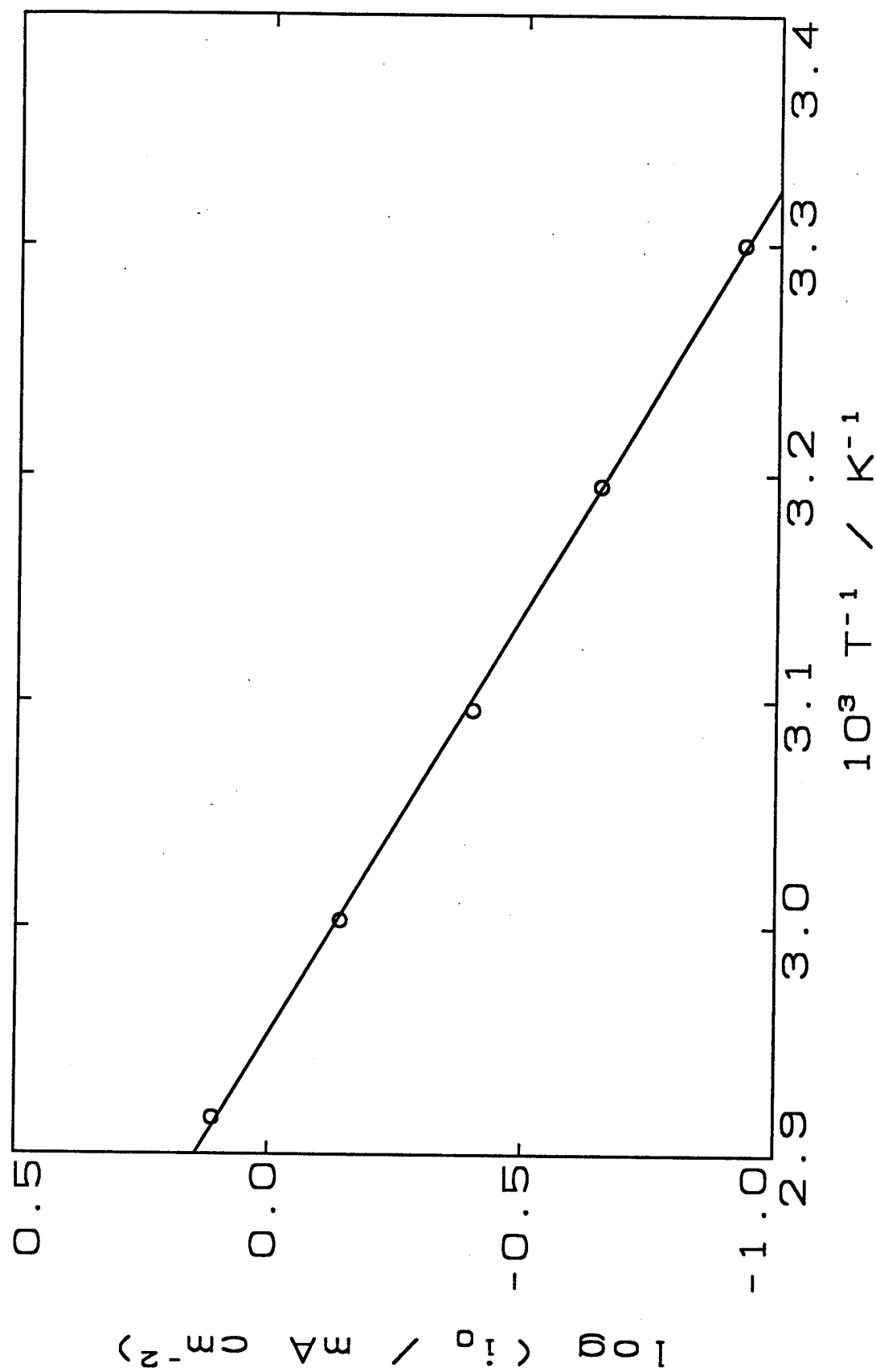
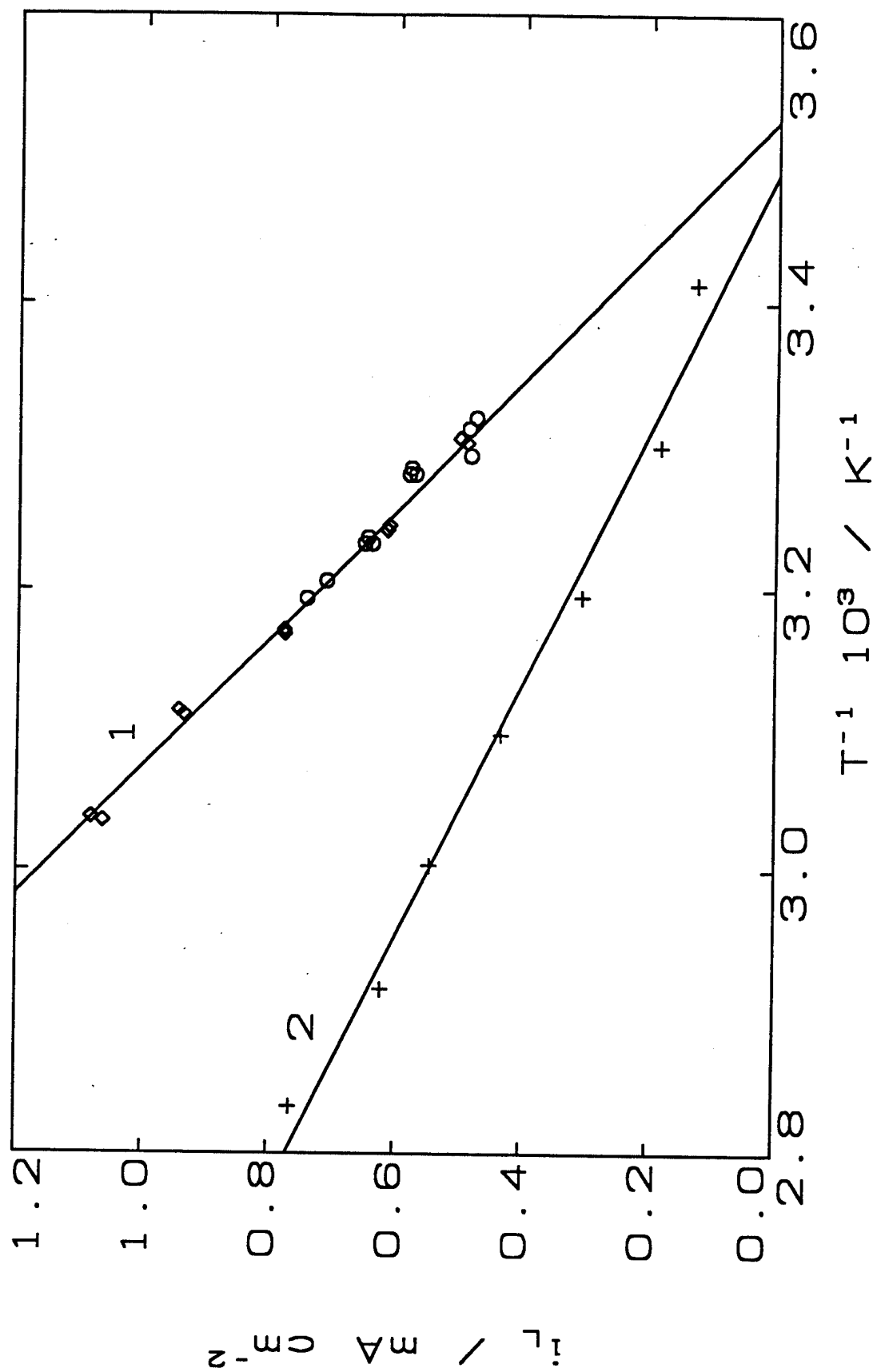
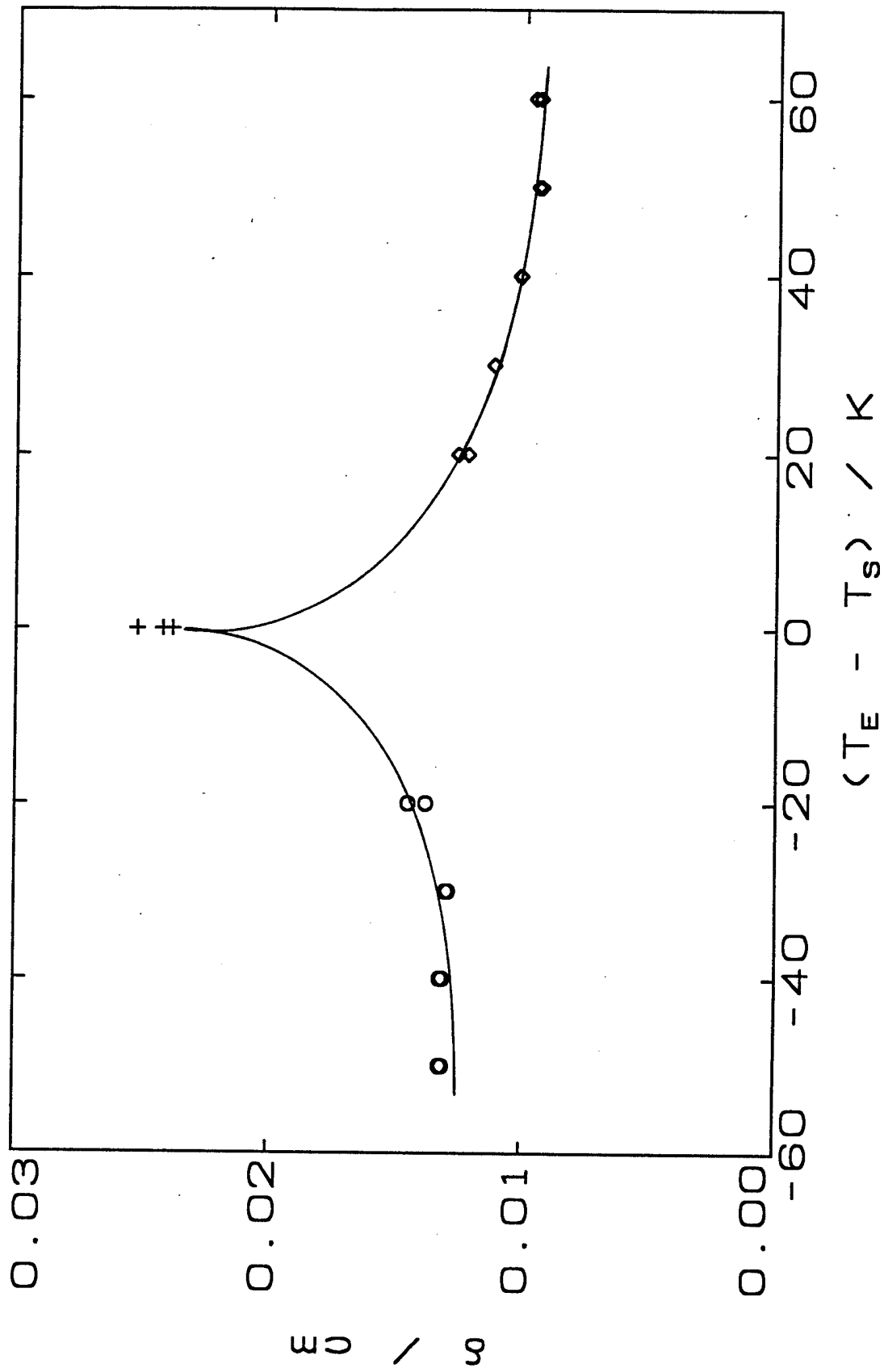


Fig. 6







Code 521
NCCOSC
San Diego, CA 92152-5000
Telephone: 619-553-2772
FAX: 619-553-6305
E-mail:
R&T Code 3133051

- Add email

*****end page 6*****

Technical Report Distribution List

Dr. Robert J. Nowak (1)*
ONR 331
800 N. Quincy St.
Arlington, VA 22217-5660

Defense Technical Information Ctr (2) **
Building 5, Cameron Station
Alexandria, VA 22314

Dr. James S. Murday (1)
Chemistry Division, NRL 6100
Naval Research Laboratory
Washington, DC 20375-5660

Dr. John Fischer (1)
Chemistry Division, Code 385
NAWCWD - China Lake
China Lake, CA 93555-6001

Dr. Peter Seligman (1)
NCCOSC - NRAD
San Diego, CA 92152-5000

Dr. James A. Gucinski (1)
NSWC Code 609
300 Highway 361
Crane, IN 47522-5001

Mr. Christopher Egan (1)
Naval Undersea Warfare Center
Division Newport
1176 Howell St.
Newport, RI 02841-1708

Dr. Carl Mueller
Naval Surface Warfare Center - White Oak
Code R36
10901 New Hampshire Ave.
Silver Springs, MD 20903-5640